

Ruthenium Complexes with Chiral Bis-Pinene Ligands: an Array of Subtle Structural Diversity

Lydia Vaquer,[†] Albert Poater,[‡] Jonathan De Tovar,[§] Jordi García-Antón,[§] Miquel Solà,[‡] Antoni Llobet,^{*,†,§} and Xavier Sala^{*,§}

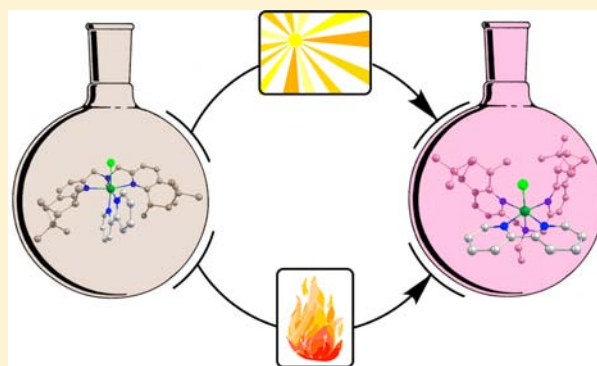
[†]Institute of Chemical Research of Catalonia (ICIQ), Avenida Països Catalans 16, E-43007 Tarragona, Spain

[‡]Departament de Química and Institut de Química Computacional, Universitat de Girona, Campus de Montilivi, E-17071 Girona, Spain

[§]Departament de Química, Universitat Autònoma de Barcelona, Cerdanyola del Vallès, 08193 Barcelona, Spain

S Supporting Information

ABSTRACT: A new chiral derivative of the *N,N*-bis(2-pyridylmethyl)ethylamine (bpea) ligand, Me-pinene[5,6]bpea [(-)-L1], has been prepared from a new aldehyde building block [Me-pinene-aldehyde, (-)-4] arising from the monoterpene chiral pool. The tridentate (-)-L1 ligand has been employed to prepare a new set of Ru–Cl complexes in combination with didentate 2,2'-bipyridine (bpy) with the general formula [RuCl((-)-L1)(bpy)]⁺. These complexes have been characterized in solution by cyclic voltammetry, UV–vis, and 1D and 2D NMR spectroscopy. Isomeric mixtures of *trans, fac*-C1a and *anti, mer*-C1c compounds are formed when (-)-L1 is reacted with a [Ru(bpy)(MeOH)Cl₃] precursor. Density functional theory calculations of all of the potential isomers of this reaction have been performed in order to interpret the experimental results in terms of electronic and steric effects and also to unravel the observed isomerization pathway between *anti, mer*-C1c and *trans, fac*-C1a.



INTRODUCTION

Today, ruthenium complexes have a variety of applications in many fields of science.¹ From a redox catalysis viewpoint, they are excellent because they enjoy a wide range of accessible oxidation states, ranging from 2– to 8+. Thus, they can be applied for both oxidative² and reductive³ transformations. Furthermore, ruthenium complexes bearing enantiopure ligands have already been used as asymmetric catalysts, giving spectacular enantiomeric excess.⁴

Within the asymmetric catalysis field, the nature of the chiral ligand plays a crucial role in the performance of the catalyst, in terms of efficiency and especially stereospecificity. However, despite the wide variety of enantiopure ligands reported so far, just a few of them have been shown to create effective asymmetric environments to a broad range of reactions and substrates.⁵ Therefore, the development of new chiral ligands that could generate “privileged” scaffolds is one of the most important issues in enantioselective catalysis by transition-metal complexes. In addition, the unraveling of the basic principles that make them “privileged” is also of paramount importance. With all this in mind, we have undertaken a project aimed at developing new chiral polypyridylic ligands with different geometries and denticities based on the monoterpene chiral pool.⁶ Their combination with metals such as manganese, iron,

and ruthenium has already led to interesting catalysts for diverse asymmetric oxidative transformations.⁷

Together with the nature of the ligands, their coordination arrangement around a given metal ion is also crucial for the final outcome of a catalytic reaction.⁸ For chiral ligands in an octahedral environment, the formation of metal complexes can lead to a large variety of isomers, especially for second-row transition metals such as ruthenium. This generates an additional challenge from a synthetic perspective in order to be able to separate and isolate individual pure isomers. Therefore, the rational ligand and complex design should be combined with appropriate synthetic methodologies in order to be successful in this type of endeavor.⁹

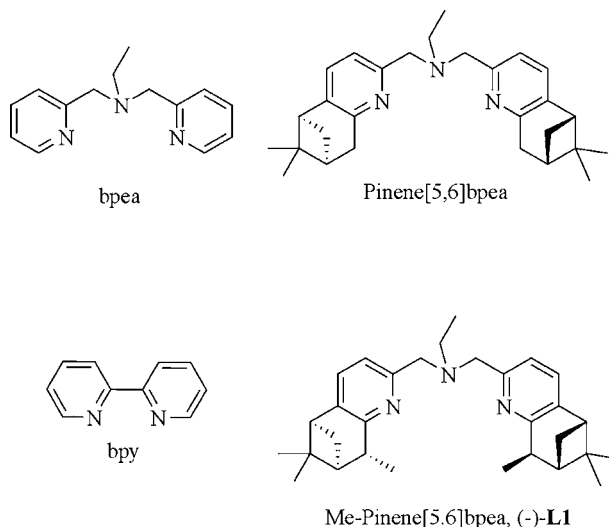
In 2008, we showed how both steric and electronic factors are key to explaining the isomeric ratios obtained when combining the *N,N*-bis(2-pyridylmethyl)ethylamine (bpea) ligand and its chiral derivative pinene[5,6]bpea (Chart 1) with *N*- and *P*-donor didentate ligands in an octahedral ruthenium(II) environment.¹⁰

Here, we further analyze this excellent platform by preparing a new diastereoselectively alkylated Me-pinene[5,6]bpea ligand [(-)-L1; Chart 1] with increased bulkiness and two new

Received: December 6, 2012

Published: April 25, 2013

Chart 1. Drawings of the Ligands Used in This Work



stereogenic centers. Ru–Cl complexes containing this ligand combined with 2,2'-bipyridine (bpy) have been prepared, thoroughly characterized, and stereoisomerically analyzed in comparison with their achiral and chiral analogues previously reported by our group.^{10,11}

EXPERIMENTAL SECTION

Materials. All reagents used in the present work were obtained from Aldrich Chemical Co. and were used without further purification. Reagent-grade organic solvents were obtained from SDS. RuCl₃·3H₂O was supplied by Alfa Aesar and was used as received.

Preparations. Pinene-furan [(-)-1]¹² and [Ru(bpy)(MeOH)Cl₃]¹³ were prepared following the procedures described in the literature.

Me-pinene-furan [(-)-2]. A solution of *n*-BuLi (26 mL, 1.6 M in hexane, 42.21 mmol) was added dropwise over a solution of diisopropylamine (6.5 mL, 46.4 mmol) in dry tetrahydrofuran (THF; 120 mL) at -40 °C. The solution of the formed LDA was brought to 0 °C in an ice bath, stirred for 30 min, and cooled again to -40 °C. A solution of the pyridine-pinene derivative (-)-1 (4.5 g, 18.8 mmol) in THF (120 mL) was added slowly for 1 h. The resulting red solution was stirred at -40 °C for 2 h. Then, methyl iodide (2.6 mL, 42.21 mmol) was added dropwise for 1 h, and the mixture was stirred overnight at room temperature. Water (310 mL) was added, and the product was extracted with dichloromethane, washed with brine, and dried with magnesium sulfate. The product was purified by column chromatography on silica gel using a mixture of hexane/ethyl acetate (95:5) as the eluent. Compound (-)-2 was obtained as a mixture of (-)-2 and Me-pinene-Me-furan (methylation on both the pinene and furan moieties) in a 10:3 ratio. This product was used without further purification in the next step. Yield: 74% (3.5 g, 13.8 mmol). ¹H NMR (400 MHz, CDCl₃): δ 7.49 (d, *J* = 1.5 Hz, 1H, H₉), 7.37 (d, *J* = 7.8 Hz, 1H, H₃), 7.20 (d, *J* = 8.0 Hz, 1H, H₄), 6.87 (d, *J* = 3.4 Hz, 1H, H₇), 6.5 (dd, *J* = 3.2 and 1.6 Hz, 1H, H₈), 3.23 (m, 1H, H₁₃), 2.75 (t, *J* = 4.8 Hz, 1H, H₁₀), 2.56 (m, 1H, H₁₄), 2.16 (m, 1H, H₁₂), 1.42 (m, 6H, H₁₅, H₁₆), 1.29 (d, *J* = 9.4 Hz, 1H, H_{14'}), 0.67 (s, 3H, H₁₇). ¹³C NMR (100 MHz, CDCl₃): δ 160.8 (C, C₂), 160.6 (C, C₁), 154.4 (C, C₆), 142.5 (CH, C₉), 140.3 (C, C₅), 133.1 (CH, C₃), 115.4 (CH, C₄), 111.8 (CH, C₈), 107.2 (CH, C₇), 47.1 (CH, C₁₀), 46.8 (CH, C₁₂), 41.4 (C, C₁₁), 38.8 (CH, C₁₃), 28.6 (CH₂, C₁₄), 26.3 (CH₃, C₁₆), 20.9 (CH₃, C₁₇), 18.3 (CH₃, C₁₅). [α]_D: -7.2 (c 1.5, CH₂Cl₂). ESI-MS: *m/z* 254.1 ([M + H]⁺), 276.1 ([M + Na]⁺).

Me-pinene-COOEt [(-)-3]. (-)-2 (23 g, 90.0 mmol) and ammonium metavanadate (1.5 g, 13.0 mmol) were mixed in water (400 mL). The mixture was heated to 65 °C, and fuming nitric acid (190 mL) was added slowly. The evolved gases were trapped by

connecting the reflux condenser to a solution of water and a mixture of aqueous NaOH (5 M) and H₂O₂ (2–3%). The solution was heated to reflux for 5 h. After distillation of the solvent under vacuum, ethanol (175 mL) and 96% sulfuric acid (64 mL) were added. The resulting solution was heated to reflux overnight. Water (800 mL) was added, and the solution was neutralized with a saturated aqueous solution of sodium carbonate. The black solid was filtered and extracted through a Soxhlet with hexane. The solvent was evaporated to obtain 14 g of (-)-3 as a yellow oil. Yield: 60% (14 g, 54 mmol). ¹H NMR (400 MHz, CDCl₃): δ 7.82 (d, *J* = 7.9 Hz, 1H, H₄), 7.29 (d, *J* = 7.9 Hz, 1H, H₃), 4.46 (m, 2H, H₁₅), 3.32 (m, 1H, H₆), 2.83 (t, *J* = 5.6 Hz, 1H, H₉), 2.58 (m, 1H, H₁₀), 2.18 (m, 1H, H₇), 1.44 (m, 9H, H₁₂, H₁₁, H₁₆), 1.30 (d, *J* = 9.1 Hz, 1H, H_{10'}), 0.63 (s, 3H, H₁₃). ¹³C NMR (100 MHz, CDCl₃): δ 165.7 (C, C₄), 157.6 (C, C₁), 146.2 (C, C₅), 145.5 (C, C₂), 133.4 (CH, C₃), 122.5 (CH, C₄), 61.6 (CH₂, C₁₅), 46.8 (CH, C₉), 40.0 (CH, C₇), 39.4 (C, C₈), 36.7 (CH, C₆), 31.5 (CH₂, C₁₀), 25.9 (CH₃, C₁₂), 21.3 (CH₃, C₁₃), 18.1 (CH₃, C₁₁), 14.4 (CH, C₁₆). [α]_D: -25.4 (c 0.94, CH₂Cl₂). ESI-MS: *m/z* 260.1 ([M + H]⁺).

Me-pinene-aldehyde [(-)-4]. (-)-3 (13.7 g, 52.8 mmol) was dissolved in anhydrous THF (200 mL), and the solution was cooled to -78 °C. LiAlH₄ (1 M in hexane, 63.4 mL) was added for a period of 20 min with a syringe pump. The resulting solution was stirred for 1 h at the same temperature. Glacial acetic acid (27 mL) was added, and the solution was left at room temperature. Hexane (400 mL) was added, and the solution was poured over water (400 mL). The solution was neutralized with a saturated solution of sodium bicarbonate, extracted with hexane, washed with water, and dried with magnesium sulfate. After collection and evaporation of the organic phases, a mixture of aldehyde (-)-4 and alcohol (-)-5 was obtained. This mixture was purified by column chromatography on silica gel. Using dichloromethane as the mobile phase, 6.8 g of (-)-4 was eluted. Yield: 60% (6.8 g, 31.6 mmol). ¹H NMR (400 MHz, CDCl₃): δ 10.04 (s, 1H, H₁₄), 7.68 (d, *J* = 7.5 Hz, 1H, H₄), 7.34 (d, *J* = 7.5 Hz, 1H, H₃), 3.27 (m, 1H, H₆), 2.86 (t, *J* = 5.3 Hz, 1H, H₉), 2.60 (m, 1H, H₁₀), 2.20 (m, 1H, H₇), 1.44 (m, 6H, H₁₁, H₁₂), 1.31 (d, *J* = 10.0 Hz, 1H, H_{10'}), 0.64 (s, 3H, H₁₃). ¹³C NMR (100 MHz, CDCl₃): δ 193.6 (COH, H₁₄), 161.8 (C, C₁), 150.8 (C, C₂), 147.4 (C, C₅), 133.3 (CH, C₃), 119.5 (CH, C₄), 47.6 (CH, C₉), 46.5 (CH, C₇), 41.4 (C, C₈), 38.7 (CH, C₆), 28.2 (CH₂, C₁₀), 26.2 (CH₃, C₁₂), 20.8 (CH₃, C₁₃), 18.1 (CH₃, C₁₁). [α]_D: -19.4 (c 0.98, CH₂Cl₂). ESI-MS: *m/z* 216.1 ([M + H]⁺), 238.1 ([M + Na]⁺).

Me-pinene-OH [(-)-5]. (-)-4 (3 g, 13.9 mmol) was dissolved in dry methanol (34 mL), and then sodium borohydride (1 g, 26.5 mmol) was added slowly. The solution was left at room temperature, and stirring was continued for 4 h. After evaporation of the solvent, dichloromethane (34 mL) and water (26 mL) were added. The product was extracted to the dichloromethane layer, washed with water, and dried with magnesium sulfate. After evaporation, 2.8 g of pure (-)-5 as a yellow solid was obtained. Yield: 92% (2.8 g, 12.9 mmol). ¹H NMR (400 MHz, CDCl₃): δ 7.17 (d, *J* = 7.5 Hz, 1H, H₃), 6.87 (d, *J* = 7.5 Hz, 1H, H₄), 4.70 (b s, 2H, H₁₄), 4.00 (b s, 1H, OH), 3.17 (m, 1H, H₆), 2.75 (t, *J* = 5.4 Hz, 1H, H₉), 2.55 (m, 1H, H₁₀), 2.15 (m, 1H, H₇), 1.43 (s, 3H, H₁₂), 1.38 (d, *J* = 7.2 Hz, 3H, H₁₁), 1.30 (d, *J* = 9.8 Hz, 1H, H_{10'}), 0.63 (s, 3H, H₁₃). ¹³C NMR (100 MHz, CDCl₃): δ 159.6 (C, C₁), 155.3 (C, C₂), 140.4 (C, C₅), 133.4 (CH, C₃), 117.0 (CH, C₄), 63.8 (CH₂, C₁₄), 46.9 (CH, C₉), 46.8 (CH, C₇), 41.3 (C, C₈), 38.6 (CH, C₆), 28.7 (CH₂, C₁₀), 26.3 (CH₃, C₁₂), 20.8 (CH₃, C₁₃), 18.1 (CH₃, C₁₁). [α]_D: -22.9 (c 1.2, CH₂Cl₂). ESI-MS: *m/z* 218.1 ([M + H]⁺), 240.1 ([M + Na]⁺).

Me-pinene-Cl [(-)-6]. (-)-5 (5.15 g, 23.7 mmol) was dissolved in dry dichloromethane (55 mL). A solution of SOCl₂ (5 mL, 71 mmol) in dry dichloromethane (44 mL) was added dropwise. The solution was kept stirring overnight. The solvent was carefully evaporated. Dichloromethane (350 mL) and an aqueous solution of sodium hydroxide (0.4 M, 666 mL) were added. The product was extracted to the dichloromethane layer, washed with water, and dried with magnesium sulfate. After evaporation, (-)-6 was obtained as a yellow oil. Yield: 88% (4.9 g, 21 mmol). ¹H NMR (400 MHz, CDCl₃): δ 7.23 (d, *J* = 7.5 Hz, 1H, H₃), 7.16 (d, *J* = 7.4 Hz, 1H, H₄), 4.68 (s, 2H,

H14), 3.20 (m, 1H, H6), 3.78 (t, $J = 5.7$ Hz, 1H, H9), 2.57 (m, 1H, H10), 2.17 (m, 1H, H7), 1.44 (s, 3H, H12), 1.40 (d, $J = 7.1$ Hz, 3H, H11), 1.32 (d, $J = 9.7$ Hz, 1H, H10'), 0.65 (s, 3H, H13). ^{13}C NMR (100 MHz, CDCl_3): δ 160.4 (C, C1), 153.1 (C, C2), 141.6 (C, C5), 134.1 (CH, C3), 119.9 (CH, C4), 47.0 (CH, C9), 46.7 (CH, C7), 46.6 (CH₂, C14), 41.3 (C, C8), 38.5 (CH, C6), 28.5 (CH₂, C10), 26.2 (CH₃, C12), 20.8 (CH₃, C13), 18.3 (CH₃, C11). $[\alpha]_{\text{D}}^{25}$: -16.4 (c 1.3, CH_2Cl_2). ESI-MS: m/z 236.1 ($[\text{M} + \text{H}]^+$).

Me-pinene[5,6]bpea [(-)-L1]. (-)-6 (2.29 mg, 9.7 μmol) was dissolved in a mixture of acetonitrile/water [1:1 (v/v), 10 mL], and 70% aqueous ethylamine (172 μL , 4.8 mmol) was added. The solution was heated to 60 °C for 5 min. Then, an aqueous solution of sodium hydroxide (10 M, 850 μL , 10.7 mmol) was added slowly. The solution was heated at 60 °C for 1 h. The product was extracted with chloroform and dried with anhydrous magnesium sulfate. The crude was purified by column chromatography of neutral alumina. Using a mixture of dichloromethane/acetone [9:1 (v/v)], (-)-L1 was eluted. Yield: 54% (1.17 g, 2.6 mmol). ^1H NMR (400 MHz, CDCl_3): δ 7.23 (d, $J = 7.7$ Hz, 2H, H2), 7.12 (d, $J = 7.7$ Hz, 2H, H3), 3.80 (s, 4H, H14), 3.15 (m, 2H, H12), 2.70 (t, $J = 5.6$ Hz, 2H, H6), 2.65 (q, $J = 7.1$ Hz, 2H, H15), 2.51 (m, 2H, H7), 2.12 (m, 2H, H8), 1.39 (s, 6H, H10), 1.35 (d, $J = 7.1$ Hz, 6H, H13), 1.28 (d, $J = 9.6$ Hz, 2H, H7'), 1.11 (t, $J = 7.1$ Hz, 3H, H16), 0.61 (s, 6H, H11). ^{13}C NMR (100 MHz, CDCl_3 , 25 °C): δ 159.8 (C, C5), 157.1 (C, C1), 139.4 (C, C4), 133.1 (CH, C3), 119.3 (CH, C2), 59.9 (CH₂, C14), 48.2 (CH₂, C15), 47.0 (2CH, C6, C8), 41.3 (C, C9), 38.7 (CH, C12), 28.7 (CH₂, C7), 26.3 (CH₃, C10), 20.9 (CH₃, C11), 18.5 (CH₃, C13), 12.3 (CH₃, C16). $[\alpha]_{\text{D}}^{25}$: -18.2 (c 1.4, CH_2Cl_2). ESI⁺-HRMS ($[\text{M} + \text{H}]^+$). Anal. Calcd for $\text{C}_{30}\text{H}_{43}\text{N}_2$: m/z 444.3373. Found: m/z 444.3398.

trans, fac-[Ru(-)-L1](bpy)ClCl (C1a) and anti, mer-[Ru(-)-L1](bpy)ClCl (C1c). To a solution of $[\text{Ru}(\text{bpy})(\text{MeOH})\text{Cl}_2]$ (53 mg, 0.134 mmol) and triethylamine (28 μL , 0.20 mmol) in dry ethanol (20 mL) was added (-)-L1 (56 mg, 0.134 mmol). The mixture was heated to reflux for 24 h in the dark. To the resulting red solution was added dry diethyl ether (50 mL). The red solution was filtered and separated from a green solid. The solution was evaporated, and the obtained solid was purified by column chromatography of alumina. Starting with dichloromethane, the polarity of the mobile phase was increased with methanol. With a mixture of dichloromethane/methanol [100:2 (v/v)], a red band was eluted. The first fractions of this band, which had a darker color and contained a mixture of C1a and C1c (11 mg), were separated. The next fractions contained pure C1a (37 mg; yield 36%). Anal. Calcd for $\text{C}_{40}\text{H}_{49}\text{ClF}_6\text{N}_3\text{PRu}$: C, 54.51; H, 5.60; N, 7.95. Found: C, 54.31; H, 5.82; N, 7.68. C1c was isolated by purification of the mixture of C1a and C1c with an alumina semipreparative thin layer chromatograph using a mixture of dichloromethane/methanol [100:2 (v/v)] as the mobile phase, obtaining 5 mg of pure C1c (yield 5%). Anal. Calcd for $\text{C}_{40}\text{H}_{49}\text{ClF}_6\text{N}_3\text{PRu}$: C, 54.51; H, 5.60; N, 7.95. Found: C, 54.42; H, 5.75; N, 7.73. C1a. ^1H NMR (500 MHz, CD_2Cl_2): δ 8.28 (d, $J = 8.0$ Hz, 1H, H4), 8.25 (d, $J = 7.8$ Hz, 1H, H5), 7.98 (d, $J = 5.5$ Hz, 1H, H1), 7.87 (t, $J = 7.3$ Hz, 1H, H3), 7.80 (t, $J = 7.3$ Hz, 1H, H6), 7.50–7.40 (4H, H9, H10, H18, H19), 7.30 (t, $J = 6.4$ Hz, 1H, H2), 7.18 (t, $J = 6.2$ Hz, 1H, H7), 6.68 (d, $J = 5.2$ Hz, 1H, H8), 5.34 (m, 1H, H21), 4.59 (d, $J = 15.6$ Hz, 1H, 28a), 4.26 (2H, H27a, H12), 4.14 (d, $J = 15.7$ Hz, 1H, H27b), 3.78 (d, $J = 15.7$ Hz, 1H, H28b), 2.95 (dt, $J = 10.3$ and 5.4 Hz, 2H, H15, H24), 2.67–2.58 (m, 1H, 29a), 2.58–2.51 (m, 2H, H14a, H23a), 2.48 (dd, $J = 13.7$ and 7.0 Hz, 1H, H29b), 2.23–2.15 (m, 4H, H13, H22, H14b, H23b), 1.76–1.68 (m, 3H, H30), 1.47 (s, 3H, H26), 1.44 (s, 3H, H16), 1.37–1.26 (m, 6H, H11, H20), 0.87 (s, 3H, H25), 0.59 (s, 3H, H17). CV (CH_2Cl_2 vs SSCE): 0.79 V. ESI⁺-HRMS ($[\text{M} - 2\text{Cl}]^{2+}$, $z = 2$). Calcd for $\text{C}_{40}\text{H}_{49}\text{N}_3\text{Ru}$: m/z 347.6532. Found: m/z 347.6518. C1c. ^1H NMR (500 MHz, CD_2Cl_2): δ 10.63 (d, $J = 5.0$ Hz, 1H, H1), 8.65 (d, $J = 7.9$ Hz, 1H, H4), 8.61 (d, $J = 6.9$ Hz, 1H, H5), 8.50 (d, $J = 5.7$ Hz, 1H, H8), 8.02–7.95 (m, 1H, H3), 7.80 (dd, $J = 11.3$ and 4.3 Hz, 1H, H6), 7.51 (ddd, $J = 7.4$, 6.0, and 1.4 Hz, 1H, H2), 7.38–7.32 (m, 1H, H7), 7.08–6.87 (m, 4H, H9, H10, H18, H19), 6.31 (d, $J = 16.6$ Hz, 1H, H28a), 5.63 (d, $J = 13.3$ Hz, 1H, H27a), 4.60 (d, $J = 16.7$ Hz, 1H, H28b), 4.52 (d, $J = 13.4$ Hz, 1H, H27b), 3.89 (dq, $J = 13.3$ and 6.6 Hz, 1H, H29a), 3.24 (dq, $J = 14.5$ and 7.3 Hz, 1H, H29b), 2.61–2.54 (m,

2H, H14a, H23a), 2.53 (dd, $J = 6.4$ and 5.5 Hz, 1H, H15), 2.49 (dd, $J = 6.4$ and 5.5 Hz, 1H, H24), 2.27–2.19 (m, 4H, H13, H22, H14b, H23b), 1.46 (s, 3H, H16), 1.42 (s, 3H, H25), 1.24 (m, 1H, H21), 1.15–1.05 (m, 3H, H30), 0.75 (d, $J = 6.9$ Hz, 3H, H20), 0.65–0.58 (m, 1H, H12), 0.59 (s, 3H, H26), 0.55 (s, 3H, H17), -0.17 (d, $J = 7.0$ Hz, 3H, H11). CV (CH_2Cl_2 , V vs SSCE): 0.83 V. The NMR assignment for C1a and C1c has been carried out in accordance with the labeling shown in Figure S15 in the Supporting Information.

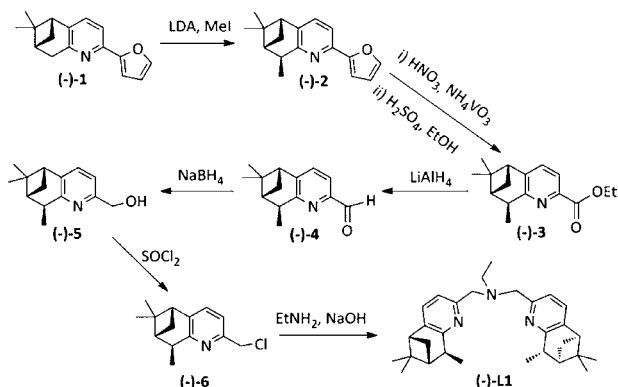
Instrumentation and Measurements. The NMR spectroscopy experiments were performed on Bruker Avance 400 and 500 Ultrashield NMR spectrometers. Samples were run in CD_2Cl_2 and CDCl_3 . Cyclic voltammetry (CV) experiments were performed on an IJ-Cambria HI-660 potentiostat using a three-electrode cell. Typical CV experiments were carried out at a scan rate of 100 mV/s. A glassy carbon electrode (2 mm diameter) was used as the working electrode, a platinum wire as the auxiliary electrode, and a saturated calomel electrode as the reference electrode. Working electrodes were polished with 0.05 μm alumina paste and washed with distilled water and acetone before each measurement. The complexes were dissolved in CH_2Cl_2 containing the necessary amount of *n*-Bu₄NPF₆ (TBAPF₆) as the supporting electrolyte to yield a 0.1 M ionic strength solution. $E_{1/2}$ values reported in this work were estimated from CV experiments as the average of the oxidative and reductive peak potentials ($E_{\text{pa}} + E_{\text{pc}}$)/2. UV–vis spectroscopy was performed on a Cary 50 (Varian) UV–vis spectrophotometer in 1 cm quartz cuvettes. Mass spectrometry analysis were performed in a mass spectrometer with time-of-flight matrix-assisted laser desorption ionization (Bruker Autoflex). Elemental analyses were performed on an EA-1108 CHNS-O elemental analyzer from Fisons Instruments (Universidad de Santiago). $[\alpha]_{\text{D}}$ was measured in a Jasco P-1030 polarimeter with symmetric angular oscillation for the sodium D line and a photomultiplier tube detector. Angular range: ± 90 °C. A Jasco spectropolarimeter (model J-715; Jasco Inc., Easton, MD) interfaced to a computer (J700 software) was used for circular dichroism (CD) measurements at a constant temperature of 25 °C, maintained by a Peltier PTC-351S apparatus (TE Technology Inc., Traverse City, MI), in CH_2Cl_2 . All spectra were recorded with 0.2 cm capped quartz cuvettes.

Computational Details. The density functional theory (DFT) calculations have been carried out with the hybrid B3PW91 functional,¹⁴ as implemented in the Gaussian 03 package.¹⁵ The Ru atoms have been represented with the quasi-relativistic effective core pseudopotentials of the Stuttgart group and the associated basis sets augmented with an f polarization function ($\alpha = 1.235$).¹⁶ The remaining atoms (C, N, P, Cl, and H) have been represented with 6-31G(d,p) basis sets.¹⁷ The B3PW91 geometry optimizations were performed without any symmetry constraints, and the nature of minima was checked by analytical frequency calculations. The energies given throughout the paper are electronic energies without zero-point-energy (ZPE) corrections (inclusion of the ZPE corrections does not significantly modify the results). These energies contain also solvent effects calculated with the polarizable continuum solvation model using ethanol as the solvent.¹⁸ These solvent effects include contributions of nonelectrostatic terms and have been estimated in single-point-energy calculations on the gas-phase-optimized structures.

RESULTS AND DISCUSSION

Synthesis and Characterization. The synthetic strategy that we have followed for preparation of the (-)-L1 ligand is outlined in Scheme 1. This strategy is based on the diastereoselective alkylation of the pyridyl-pinene-aldehyde [(-)-4; Scheme 1]. The latter is a very convenient chiral building block intermediate for the synthesis of a wide variety of polypyridylic ligands via simple Schiff-base chemistry, as we have previously shown with related (nonalkylated) aldehyde scaffolds.^{7b–d} The synthetic pathway followed started with the furan derivative (-)-I developed by Bernhard and co-workers¹² (Scheme 1). Methylation of (-)-I at the methylene group

Scheme 1. Synthetic Pathway for the (–)-L1 Ligand



adjacent to the pyridine ring employing LDA and methyl iodide took place in a diastereoselective manner to form (–)-2 in good yield (74%).¹⁹

The next step consisted of the oxidative degradation of the furan substituent by employing a mixture of nitric acid and ammonium metavanadate. The carboxylic acid formed is esterified in situ with sulfuric acid in ethanol, and compound (–)-3 is obtained in 60% yield. Reduction of the obtained ester (–)-3 with LiAlH₄ resulted in formation of the desired (–)-4 and (–)-5 as minor byproducts. The two products were separated by column chromatography on silica gel (see the Experimental Section for further details), obtaining (–)-4 in 60% yield. The slow and careful addition of NaBH₄ was then employed for the almost quantitative reduction of (–)-4 to alcohol (–)-5 (92% yield). The subsequent formation of (–)-6 in quantitative yield was obtained by the slow addition of SOCl₂ to (–)-5. Finally, a double nucleophilic attack of ethylamine over (–)-6 led to formation of the desired (–)-L1 ligand (54% yield).

(–)-L1 was characterized by NMR (1D and 2D), ESI-MS, and optical polarimetry (see the Experimental Section and Figures S16–S21 in the Supporting Information). The ¹H NMR spectrum of (–)-L1 is presented in Figure 1, together

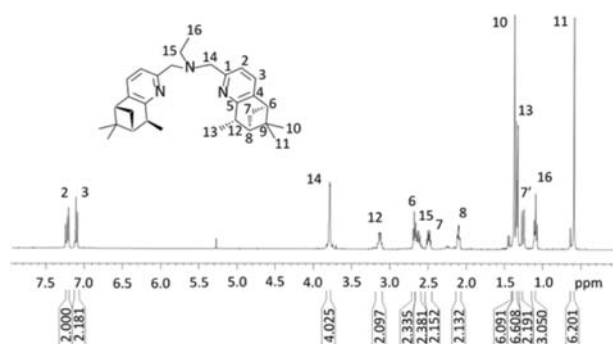


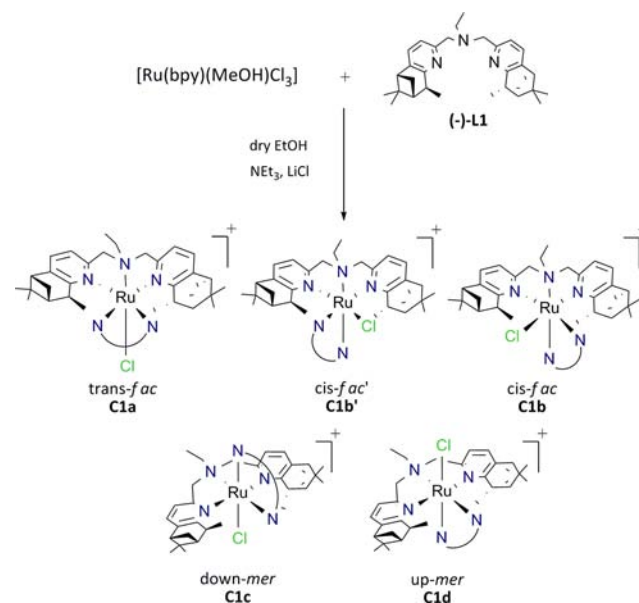
Figure 1. ¹H NMR spectrum of (–)-L1 and its corresponding labeling scheme.

with its corresponding labeling scheme. C₂ symmetry is observed in solution, and thus the two pyridine-pinene moieties are equivalent. This leads to 16 resonances that were unequivocally assigned to the corresponding protons after analysis of the homo- and heteronuclei bidimensional spectra.

Ru–Cl complexes were then prepared by employing [Ru(bpy)(MeOH)Cl₃] as the metal precursor. The sequence of ligand addition to the Ru metal center is reversed here with

regard to the previously related complexes containing the pinene[5,6]bpea and bpea ligands reported earlier,^{10,11} and actually this turns out to be essential in this particular case for preparation of the desired compounds. Attempts to coordinate the bpy ligand to a typical [Ru((–)-L1)Cl₃] intermediate were always unfruitful because of the increased bulkiness of the (–)-L1 ligand. Therefore, we used a solution of [Ru(bpy)(MeOH)Cl₃] in dry ethanol and added (–)-L1 and triethylamine to generate the corresponding complexes (Scheme 2).

Scheme 2. Synthetic Procedure and Potential Isomers of C1



The substitution of one methanol (MeOH) and two chlorido ligands by a flexible^{10,20} C₂-symmetric tridentate N-donor ligand such as (–)-L1 can potentially lead to a wide range of stereoisomers, as shown in Scheme 2. The flexibility of the mentioned ligands will allow them to coordinate in a facial or meridional manner around the octahedral Ru^{II} d⁶ metal center.

When the tridentate ligands act in a facial manner, then *cis* and *trans* isomers can be obtained depending on whether the Ru–Cl bond is *cis* or *trans* to the Ru–N_{aliphatic} bond, respectively. In the particular case of a *cis*/*fac* configuration, two possible isomers can be obtained and are depicted in Scheme 2 as C1b and C1b'. When the tridentate ligands act in a meridional fashion, two possibly isomers can be obtained depending on the relative orientation of the Ru–Cl bond with regard to the ethyl group of the aliphatic amine. These isomers are thus named *anti*,*mer*-C1c and *syn*,*mer*-C1d (Scheme 2).

Reaction of the [Ru(bpy)(MeOH)Cl₃] complex with (–)-L1 in dry ethanol at reflux for 24 h generates a mixture of complexes. A careful ¹H NMR analysis of the crude revealed the presence of two major complexes: *trans*,*fac*-C1a and *anti*,*mer*-C1c in a 84:16 ratio. Additionally, the NMR also showed the presence of small amounts of a third complex that could not be identified but that, on the basis of DFT, could be potentially assigned to C1d (*vide infra*). Overall we managed to account for 78% yield.

It is worth mentioning here that the introduction of two extra methyl groups to the pinene[5,6]bpea ligand [Chart 1; (–)-L1] produces an enhancement of the steric effects close to the metal center in such a way that the number of isomers obtained is now substantially lower.¹⁰ For this reason, in the present case,

we manage to obtain *trans, fac*-**C1a** as the major product. This was also the case for the achiral bpea ligand (Chart 1), where the main isomer obtained was *trans, fac*-[Ru(bpea)(bpy)Cl]⁺ (**C3a**).¹¹ Isolation of both **C1a** and **C1c** (Scheme 2) as pure isomers was accomplished by combining column chromatography and semipreparative thin layer chromatography (TLC), both having alumina as the solid phase. Elution of the former with 50:1 dichloromethane/methanol allowed us to obtain pure **C1a** (36% yield) and a mixture of **C1a** and **C1c**. Semipreparative TLC using the same elution conditions finally allowed us to isolate pure **C1c** (5% yield). In Figure S15 in the Supporting Information, the ¹H NMR of the reaction crude is plotted together with the ¹H NMR of the isolated isomers **C1a** and **C1c**. For these types of complexes, 1D and 2D NMR has been shown to be an extremely powerful tool to unambiguously identify and characterize the isolated isomers (Scheme 2). In particular, the chemical shift of the CH₂-N moieties is indicative of the presence of a facial or meridional disposition of (–)-**L1**. A chemical shift for the CH₂-N unit of around 6 ppm is indicative of meridional geometry, whereas a shift of more than 1 ppm to higher fields indicates facial coordination.²⁰ For **C1a**, this chemical shift is 4 ppm and thus is a clear indication of the facial geometry of (–)-**L1** in this compound. This is further corroborated by the absence of shifted bpy protons because of the fact that the bpy ligand is situated perpendicular to the Ru–Cl bond (see Figures S15 and S22 in the Supporting Information). 2D NOESY experiments allowed us to distinguish between the three potential facial isomers (**C1a**, **C1b**, and **C1b'**; Scheme 2). Two interactions between bpy and (–)-**L1** protons, H8 with H15 and H1 with H20, allow identification of the *trans, fac*-**C1a** isomer (Figure S22 in the Supporting Information). The assignment of the *anti, mer*-**C1c** isomer is based on three key observations. First, the chemical shift of CH₂-N at around 6 ppm suggests a meridional conformation.²⁰ Second, a deshielded doublet shifted to low fields (H1 of the bpy ligand in Figure S27 in the Supporting Information) reveals the presence of the Ru–Cl bond parallel to the bpy plane. Finally, a NOE interaction between H26a of (–)-**L1** and H8 of the bpy ligand (Figure S27 in the Supporting Information) clearly supports the presence of the *anti, mer*-**C1c** isomer.

The electrochemical properties of **C1a** and **C1c** were investigated by means of CV in dichloromethane (Figure S32 in the Supporting Information). *trans, fac*-**C1a** and *anti, mer*-**C1c** isomers exhibit chemically reversible and electrochemically quasi-reversible waves centered at $E_{1/2} = 0.79$ V ($\Delta E_p = 90$ mV) and 0.83 V ($\Delta E_p = 110$ mV), respectively. Therefore, σ donation of the tertiary amine of the (–)-**L1** ligand seems to be more effective when the N_{aliphatic}-Ru bond is *trans* to the Ru–Cl bond, decreasing the Ru^{III/II} redox potential by roughly 40 mV. A similar cathodic shift in the redox potentials is observed in a comparison of related meridional versus facial isomers of achiral bpea complexes, as has been previously reported.^{20a}

In the presence of light and in a CH₂Cl₂ solution, **C1c** is not stable and isomerizes toward the *trans, fac* isomer **C1a**. This transformation has been followed by ¹H NMR and is shown in Figure 2. After 24 h of irradiation, the *anti, mer* isomer **C1c** is no longer present in solution. The isomerization kinetics has also been followed by UV–vis spectroscopy (Figure S33 in the Supporting Information). A decrease in the absorbance at 395, 480, and 500 nm and the appearance of a new band at 530 nm are observed together with clean isosbestic points, indicating a neat interconversion between the two species. Under the same

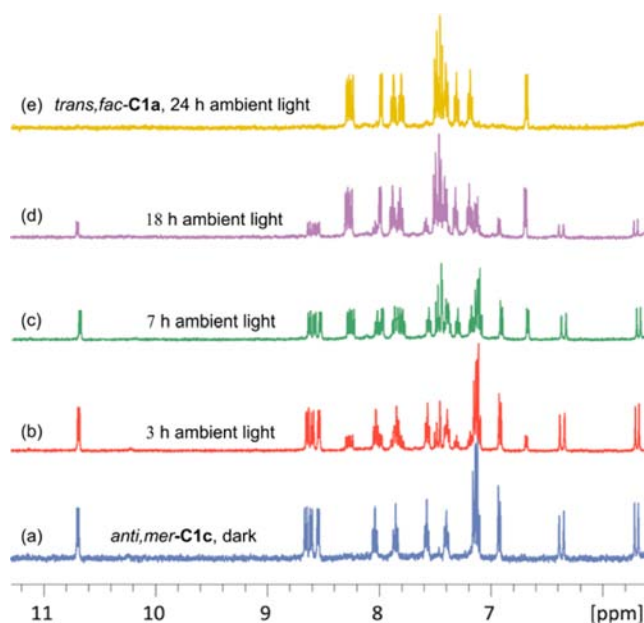


Figure 2. ¹H NMR spectra (aromatic region, CD₂Cl₂) monitoring the isomerization process of *anti, mer*-**C1c** to *trans, fac*-**C1a** triggered by ambient light irradiation.

conditions, but in the absence of light, there is no transformation at all, as indicated by UV–vis and ¹H NMR spectroscopy.

The isomerization of **C1c** → **C1a** can also be thermally promoted in the dark, by refluxing a solution of the former complex in 1,2-dichloroethane. In this case, the reaction is much slower, taking 168 h to proceed (Figure S35 in the Supporting Information).

The thermal *mer/fac* isomerization of a bpea ligand bound to a Ru^{II} metal ion was already described by us for the [Ru(Cl)₂(bpea)(DMSO)] complex.^{20b} In this case, a dissociative mechanism was proposed, in which one of the chlorido ligands was removed as the initial step. In order to gain a deeper understanding of this kind of process and assess the influence of the steric and electronic effects imposed by the ligands over the isomerization mechanism, DFT calculations were carried out for the **C1c** → **C1a** thermal process, where the facial isomer **C1a** is slightly more stable (1.3 kcal/mol) than the meridional isomer **C1c**. Two possible dissociative mechanisms were proposed as the initial hypothesis: a first one based on the dissociation of a pyridylic arm of the (–)-**L1** ligand (pathway a, Figure 3) and a second one based on the removal of the chlorido ligand (pathway b, Figure 3). The energies of the different calculated species involved in both mechanisms are represented in Figure 3. Following pathway a, one pyridyl ring of (–)-**L1** is first decoordinates to reach the transition state **TSI** by means of 34.4 kcal/mol. On the other hand, release of a chlorido ligand from **C1c** (pathway b) leads first to the formation of intermediate **II** and subsequently to pentacoordinated transition state **TSIII** through a highly energetically demanding reorganization process (44.1 kcal/mol). Further ligand reorganization allows the gathering of species **III** with the already facial coordination of (–)-**L1**. In general, decoordination of an “arm” of a chelating ligand is disfavored with regard to decoordination of a monodentate ligand.^{20b} In this case, the steric hindrance exerted by the pinene moieties precludes reorganization of the pentacoordinated species up to

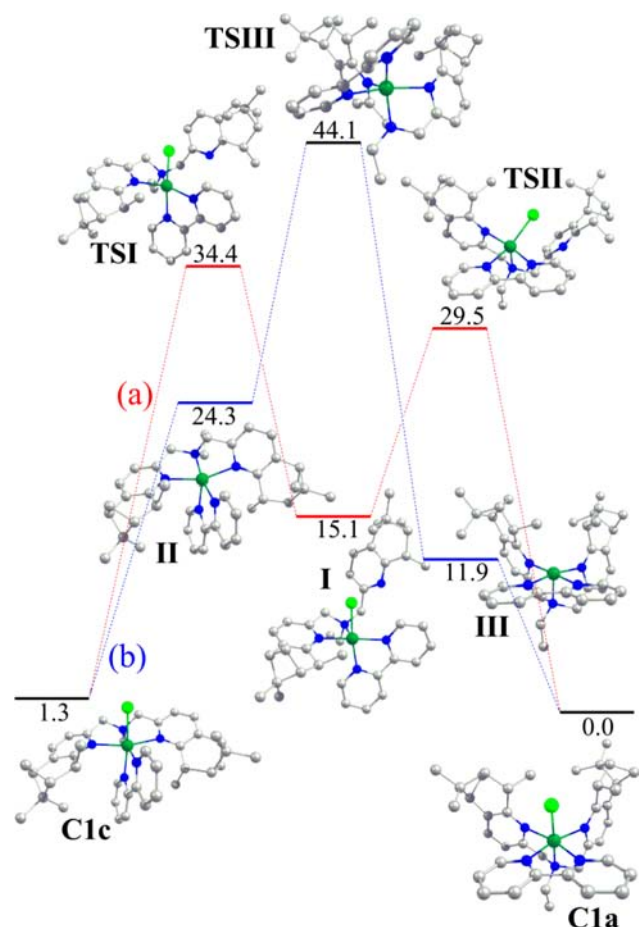


Figure 3. Relative energy diagram for the B3PW91 C1c → C1a isomerization.

44.1 kcal/mol, hampering the viability of this mechanism. However, decooordination of one pyridyl ring gives rise to a much more flexible intermediate, less sterically hindered and easier to reorganize to its facial form. These steric arguments would also explain why in the case of the previously reported [Ru(Cl)₂(bpea)(DMSO)] complex, in which no bulky ligands are used, the proposed *mer*-to-*fac* isomerization mechanism was based on the initial removal of a chlorido ligand.^{20b}

Stereoisomeric Analysis. DFT calculations were performed for the five potential isomers of C1, and their relative energy diagram is shown in Figure 4a. In the same figure, the relative energy diagram is compared with the ones reported recently for the two analogous complexes [Ru(pinene[5,6]-bpea)(bpy)Cl]⁺ (C2; Figure 4b) and ([Ru(bpea)(bpy)Cl]⁺ (C3; Figure 4c), containing respectively nonalkylated and achiral bpea scaffolds.¹⁰ Selected bond distances and angles are collected in Table S1 in the Supporting Information for all of the optimized structures of C1 together with reported data for C2 and C3, for purposes of comparison. To simplify the structural discussion for these complexes, the plane nearly perpendicular to the Ru–X bond (X = monodentate ligand) will be considered to be the equatorial plane.

For the C3 complexes containing the achiral bpea ligand, only the C3a isomer is obtained experimentally. This is due to the absence of a strong steric interaction and the presence of hydrogen bonding between the chlorido ligand and the CH groups situated in the α position with regard to the N atoms of the bpea pyridyl rings (see Figure 4c).¹⁰ Introduction of a

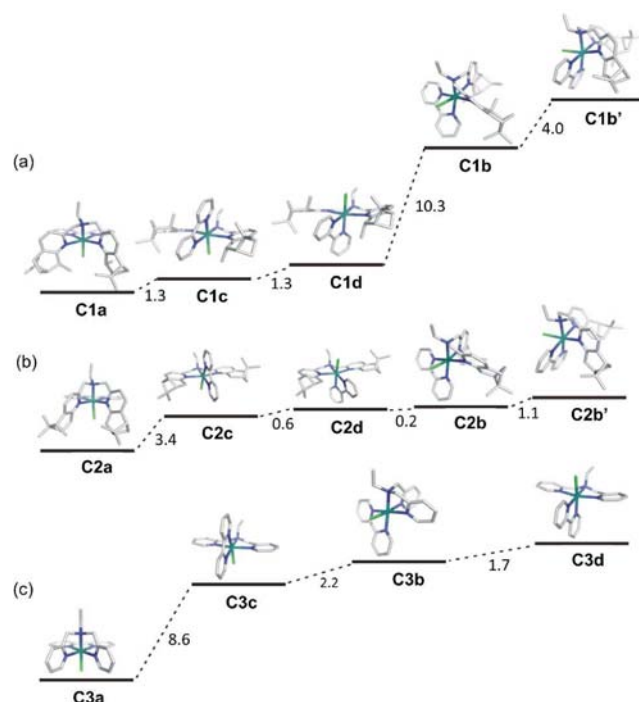


Figure 4. Relative energy diagram for the B3PW91-optimized geometries of the cationic moieties of (a) C1a–C1d, (b) C2a–C2d, and (c) C3a–C3d. Energies are given in kcal/mol. Color codes: ruthenium, light blue; chlorine, green; nitrogen, blue; carbon, gray.

pinene moiety in the 5 and 6 positions of the pyridylic bpea rings (pinene[5,6]bpea, Chart 1) produces large steric interactions and removes the potential hydrogen bonding mentioned above. As a consequence of this, the relative energies of the potential isomers are relatively similar and thus synthetically we obtain a mixture of isomers: *trans, fac*-C2a, *cis, fac*-C2b/C2b', and *syn, mer*-C2d (Figure 4b).¹⁰ Finally, the double alkylation of the pinene moieties in (–)-L1 provokes a further increase of the steric hindrance, clearly destabilizing the *cis, fac* isomers C1b and C1b' by 12.9 and 16.9 kcal/mol over *trans, fac*-C1a, respectively (Figure 4a), which is the more stable isomer in the present case. Strong repulsive steric interactions between the bpy ligand and one of the bulky Me-pinene groups of (–)-L1, both occupying the equatorial plane, are responsible for this energy increase. As a consequence of this, C1b/C1b' isomers present a large distortion of the octahedral geometry (see Figure 4a and Table S1 in the Supporting Information). An indication of the degree of this octahedral distortion is offered by the dihedral angles between the two pyridyl rings of (–)-L1. For C1b, this angle is 68.4°, whereas for C1b', it is 71.4°, while for an ideal geometry, these rings should be almost coplanar. This highly disfavored steric situation explains why these *cis, fac* isomers are not observed experimentally. In sharp contrast, the steric constraints clearly decrease when (–)-L1 coordinates meridionally to the Ru metal center. Now *anti, mer*-C1c and *syn, mer*-C1d are only 1.3 and 2.6 kcal/mol above the more stable *trans, fac*-C1a isomer. This enhanced stability of the *mer* isomers with regard to the *cis, fac* ones is due to the reduced steric hindrance between the bpy ligand and the pinene groups in this new geometry, as can be clearly observed in Figure 4. Nevertheless, there is still some remaining hindrance between the bpy pyridyl group *trans* to the chlorido ligand and (–)-L1, as can be inferred from the increased Ru–N_{bpy} distance from the typical 2.05 Å up to the 2.10 Å calculated for this isomer

(see, for instance, Ru–N4/N5 in Table S1 in the Supporting Information). Finally, the *trans,trans* disposition of (–)-L1 has the lowest steric hindrance between the bpy and pinene groups and thus becomes the most stable isomer. This is in total agreement with the fact that it is by far the major isomer obtained experimentally.

In conclusion, we have prepared a new chiral dialkylated pyridyl-pineno-fused aldehyde building block, (–)-4, which has been employed in the preparation of a new enantiopure derivative of the bpea ligand, (–)-L1. The combination of the latter with a [RuCl(bpy)]⁺ subunit afforded *trans,trans*-C1a as the major product together with *anti,mer*-C1c in much lesser amounts. The reduced isomeric mixture obtained here (when compared with the one previously reported for Ru–Cl complexes bearing a nonalkylated pineno-fused bpea ligand, C2) arises from the strong destabilization of *cis,trans*-C1b/C1b' isomers. As shown by their highly distorted DFT-calculated structures, the large steric repulsions between one of the bulky Me-pinene groups and a bpy pyridyl moiety occupying the equatorial plane produce the observed energy increase. Furthermore, the calculated thermodynamic instability of the *anti,mer* isomer versus its *trans,trans* counterpart is experimentally confirmed by the C1c → C1a thermo- and photoisomerization processes observed. Here again, for the thermal case, steric arguments (lower ligand reorganization energies) support the initial dissociation of a bpea pyridylic arm, as described by DFT, instead of a Ru–Cl decoordination pathway.

■ ASSOCIATED CONTENT

■ Supporting Information

Computational details and spectroscopic (1D and 2D NMR) and electrochemical measurements for the reported complexes, UV–vis spectra of the C1c → C1a isomerization process, and CD spectrum of C1a. This material is available free of charge via the Internet at <http://pubs.acs.org>.

■ AUTHOR INFORMATION

■ Corresponding Author

*E-mail: allobet@iciq.es (A.L.), xavier.sala@uab.cat (X.S.).

■ Notes

The authors declare no competing financial interest.

■ ACKNOWLEDGMENTS

Support from MINECO (Grants CTQ2011-26440, CTQ2010-21497, and CTQ2011-23156/BQU) is gratefully acknowledged. Financial help from the DIUE of the Generalitat de Catalunya (Projects 2009SGR637 and XRQTC) and the FEDER fund (European Fund for Regional Development) for Grant UNGI08-4E-003 is acknowledged. L.V. is grateful for the award of a FI doctoral grant from AGAUR. A.P. is grateful to the European Commission (Grant CIG09-GA-2011-293900), Spanish MICINN (Ramón y Cajal Contract RYC-2009-05226), and Generalitat de Catalunya (Grant 2011BE100793). Support for the research of M.S. was received through the ICREA Academia 2009 prize for excellence in research funded by the DIUE of the Generalitat de Catalunya.

■ REFERENCES

(1) (a) Baranoff, E.; Collin, J.-P.; Furusho, J.; Furusho, Y.; Laemmel, A.-C.; Sauvage, J.-P. *Inorg. Chem.* **2002**, *41*, 1215–1222. (b) Kelley, S. O.; Barton, J. K. *Science* **1999**, *283*, 375–381. (c) Schuster, G. B. *Acc. Chem. Res.* **2000**, *33*, 253–260. (d) Venturi, M.; Balzani, V.; Ballardini, R.; Credi, A.; Gandolfi, M. T. *Int. J. Photoenergy* **2004**, *6*, 1–10.

(e) Weatherly, S. C.; Yang, I. V.; Thorp, H. H. *J. Am. Chem. Soc.* **2001**, *123*, 1236–1237.

(2) (a) Keene, F. R. *Coord. Chem. Rev.* **1999**, *187*, 121–149. (b) Csajernyik, G.; Ell, A. H.; Fadini, L.; Pugin, B.; Bäckvall, J.-E. *J. Org. Chem.* **2002**, *67*, 1657–1662. (c) Bäckvall, J.-E., Ed. *Modern Oxidation Methods*, 2nd Completely Revised; Wiley-VCH Verlag GmbH & Co. KGaA: Berlin, 2010. (d) Stultz, L. K.; Binstead, R. A.; Reynolds, M. S.; Meyer, T. J. *J. Am. Chem. Soc.* **1995**, *117*, 2520–2532. (e) Sala, X.; Romero, I.; Rodríguez, M.; Escriche, L.; Llobet, A. *Angew. Chem., Int. Ed.* **2009**, *48*, 2842–2852. (f) Concepcion, J. J.; Jurss, J. W.; Templeton, J. L.; Meyer, T. J. *J. Am. Chem. Soc.* **2008**, *130*, 16462–16463. (g) Sala, X.; Poater, A.; Romero, I.; Rodríguez, M.; Llobet, A.; Solans, X.; Parella, T.; Santos, T. M. *Eur. J. Inorg. Chem.* **2004**, 612–618. (h) Duan, L.; Bozoglian, F.; Mandal, S.; Stewart, B.; Privalov, T.; Llobet, A.; Sun, L. *Nat. Chem.* **2012**, *4*, 418–423.

(3) (a) Mashima, K.; Kusano, K.-h.; Sato, N.; Matsumura, Y.-i.; Nozaki, K.; Kumobayashi, H.; Sayo, N.; Hori, Y.; Ishizaki, T. *J. Org. Chem.* **1994**, *59*, 3064–3076. (b) Ohta, T.; Miyake, T.; Seido, N.; Kumobayashi, H.; Takaya, H. *J. Org. Chem.* **1995**, *60*, 357–363. (c) Arai, N.; Azuma, K.; Nii, N.; Ohkuma, T. *Angew. Chem., Int. Ed.* **2008**, *47*, 7457–7460. (d) Federsel, C.; Jackstell, R.; Beller, M. *Angew. Chem., Int. Ed.* **2010**, *49*, 6254–6257. (e) Jessop, P. G. *Handb. Homogeneous Hydrogenation* **2007**, *1*, 489–511. (f) Jessop, P. G.; Joo, F.; Tai, C. C. *Coord. Chem. Rev.* **2004**, *248*, 2425–2442. (g) Planas, N.; Ono, T.; Vaquer, L.; Miro, P.; Benet-Buchholz, J.; Gagliardi, L.; Cramer, C. J.; Llobet, A. *Phys. Chem. Chem. Phys.* **2011**, *13*, 19480–19484.

(4) (a) Tse, M. K.; Bhor, S.; Klawonn, M.; Anikumar, G.; Haijun, J.; Doebler, C.; Spannenbert, A.; Maegerlein, W.; Hugl, H.; Beller, M. *Chem.—Eur. J.* **2006**, *12*, 1855–1874. (b) Tse, M.; Bhor, S.; Klawonn, M.; Anikumar, G.; Haijun, J.; Anke, S.; Doebler, C.; Maegerlein, W.; Hugl, H.; Beller, M. *Chem.—Eur. J.* **2006**, *12*, 1875–1888. (c) Serrano, I.; Rodríguez, M.; Romero, I.; Llobet, A.; Parella, T.; Campelo, J. M.; Luna, D.; Marinas, J. M.; Benet-Buchholz, J. *Inorg. Chem.* **2006**, *45*, 2644–2651. (d) Sala, X.; Plantalech, E.; Romero, I.; Rodríguez, M.; Llobet, A.; Poater, A.; Duran, M.; Solà, M.; Jansat, S.; Gómez, M.; Parella, T.; Stoeckli-Evans, H.; Benet-Buchholz, J. *Chem.—Eur. J.* **2006**, *12*, 2798–2807. (e) Sala, X.; Serrano, I.; Rodríguez, M.; Romero, I.; Llobet, A.; van Leeuwen, P. W. N. M. *Catal. Commun.* **2009**, *9*, 117–119. (f) Chatterjee, D. *Coord. Chem. Rev.* **2008**, *252*, 176–198.

(5) (a) Pfaltz, A.; Drury, W. J., III. *Proc. Natl. Acad. Sci. U.S.A.* **2004**, *101*, 5723–5726. (b) Yoon, T. P.; Jacobsen, E. N. *Science* **2003**, *299*, 1699–1693.

(6) Sala, X.; Rodríguez, A. M.; Rodríguez, M.; Romero, I.; Parella, T.; von Zelewsky, A.; Llobet, A.; Benet-Buchholz, J. *J. Org. Chem.* **2006**, *71*, 9283–9290.

(7) (a) Rich, J.; Rodríguez, M.; Romero, I.; Vaquer, L.; Sala, X.; Llobet, A.; Corbella, M.; Collomb, M.-N.; Fontrodona, X. *Dalton Trans.* **2009**, 8117–8126. (b) Gómez, L.; García-Bosch, I.; Company, A.; Sala, X.; Fontrodona, X.; Ribas, X.; Costas, M. *Dalton Trans.* **2007**, 5539–5545. (c) Gómez, L.; García-Bosch, I.; Company, A.; Benet-Buchholz, J.; Polo, A.; Sala, X.; Ribas, X.; Costas, M. *Angew. Chem., Int. Ed.* **2009**, *48*, 5720–5723. (d) Rich, J.; Rodríguez, M.; Romero, I.; Fontrodona, X.; van Leeuwen, P. W. N. M.; Freixa, Z.; Sala, X.; Poater, A.; Solà, M. *Eur. J. Inorg. Chem.* **2013**, 1213–1224.

(8) For instance, see: (a) Aharoni, A.; Vidavsky, Y.; Diesendruck, C. E.; Ben-Asuly, A.; Goldberg, I.; Lemcoff, N. G. *Organometallics* **2011**, *30*, 1607–1615. (b) Fachetti, G.; Cesarotti, E.; Pellizzoni, M.; Zerla, D.; Rimoldi, I. *Eur. J. Inorg. Chem.* **2012**, 4365–4370. (c) Ciancaleoni, G.; Fraldi, N.; Cipullo, R.; Busico, V.; Maccioni, A.; Budzelaar, P. H. M. *Macromolecules* **2012**, *45*, 4046–4053. (d) Roeser, S.; Farras, P.; Bozoglian, F.; Martínez-Belmonte, M.; Benet-Buchholz, J.; Llobet, A. *ChemSusChem* **2011**, *4*, 197–207. (e) Sens, C.; Rodríguez, M.; Romero, I.; Llobet, A.; Parella, T.; Sullivan, B. P.; Benet-Buchholz, J. *Inorg. Chem.* **2003**, *42*, 2040–2048. (f) Serrano, I.; López, M. I.; Ferrer, I.; Poater, A.; Parella, T.; Fontrodona, X.; Solà, M.; Llobet, A.; Rodríguez, M.; Romero, I. *Inorg. Chem.* **2011**, *50*, 6044–6054.

(9) (a) von Zelewsky, A. *Stereochemistry of Coordination Compounds*; Wiley: New York, 1998. (b) von Zelewsky, A. *Coord. Chem. Rev.* **1999**, *190–192*, 811–825.

(10) Sala, X.; Poater, A.; von Zelewsky, A.; Parella, T.; Fontrodona, X.; Romero, I.; Solà, M.; Rodríguez, M.; Llobet, A. *Inorg. Chem.* **2008**, *47*, 8016–8024.

(11) Rodríguez, M.; Llobet, A.; Romero, I.; Deronzier, A.; Biner, M.; Parella, T.; Stoeckli-Evans, H. *Inorg. Chem.* **2001**, *40*, 4150–4156.

(12) Sauer, A. L.; Ho, D. M.; Bernhard, S. *J. Org. Chem.* **2004**, *69*, 8910–8915.

(13) Eskelinen, E.; Da Costa, P.; Haukka, M. *J. Electroanal. Chem.* **2005**, *579*, 257–265.

(14) (a) Becke, A. D. *J. Chem. Phys.* **1993**, *98*, 5648–5652.

(b) Perdew, J. P.; Wang, Y. *Phys. Rev. B* **1992**, *45*, 13244–13249.

(15) Frisch, M. J.; Trucks, G. W.; Schlegel, H. B.; Scuseria, G. E.; Robb, M. A.; Cheeseman, J. R.; Montgomery, J. A., Jr.; Vreven, T.; Kudin, K. N.; Burant, J. C.; Millam, J. M.; Iyengar, S. S.; Tomasi, J.; Barone, V.; Mennucci, B.; Cossi, M.; Scalmani, G.; Rega, N.; Petersson, G. A.; Nakatsuji, H.; Hada, M.; Ehara, M.; Toyota, K.; Fukuda, R.; Hasegawa, J.; Ishida, M.; Nakajima, T.; Honda, Y.; Kitao, O.; Nakai, H.; Klene, M.; Li, X.; Knox, J. E.; Hratchian, H. P.; Cross, J. B.; Bakken, V.; Adamo, C.; Jaramillo, J.; Gomperts, R.; Stratmann, R. E.; Yazyev, O.; Austin, A. J.; Cammi, R.; Pomelli, C.; Ochterski, J. W.; Ayala, P. Y.; Morokuma, K.; Voth, G. A.; Salvador, P.; Dannenberg, J. J.; Zakrzewski, V. G.; Dapprich, S.; Daniels, A. D.; Strain, M. C.; Farkas, O.; Malick, D. K.; Rabuck, A. D.; Raghavachari, K.; Foresman, J. B.; Ortiz, J. V.; Cui, Q.; Baboul, A. G.; Clifford, S.; Cioslowski, J.; Stefanov, B. B.; Liu, G.; Liashenko, A.; Piskorz, P.; Komaromi, I.; Martin, R. L.; Fox, D. J.; Keith, T.; Al-Laham, M. A.; Peng, C. Y.; Nanayakkara, A.; Challacombe, M.; Gill, P. M. W.; Johnson, B.; Chen, W.; Wong, M. W.; Gonzalez, C.; Pople, J. A. *Gaussian 03*, revision C.02; Gaussian, Inc.: Wallingford, CT, 2004.

(16) (a) Andrae, D.; Haussermann, U.; Dolg, M.; Stoll, H.; Preuss, H. *Theor. Chim. Acta* **1990**, *77*, 123–141. (b) Bergner, A.; Dolg, M.; Kuchle, W.; Stoll, H.; Preuss, H. *Mol. Phys.* **1993**, *80*, 1431–1444.

(17) (a) Hehre, W. J.; Ditchfield, R.; Pople, J. A. *J. Chem. Phys.* **1972**, *56*, 2257–2261. (b) Hariharan, P. C.; Pople, J. A. *Theor. Chim. Acta* **1973**, *28*, 213–222.

(18) (a) Barone, V.; Cossi, M. *J. Phys. Chem. A* **1998**, *102*, 1995–2001. (b) Tomasi, J.; Persico, M. *Chem. Rev.* **1994**, *94*, 2027–2094.

(19) (a) Loetscher, D.; Rupprecht, S.; Collomb, P.; Belsler, P.; Viebrock, H.; von Zelewsky, A.; Burger, P. *Inorg. Chem.* **2001**, *40*, 5675–5681. (b) Malkov, A. V.; Bell, M.; Castelluzzo, F.; Kocovski, P. *Org. Lett.* **2005**, *7*, 3219–3222.

(20) (a) Mola, J.; Rodríguez, M.; Romero, I.; Llobet, A.; Parella, T.; Poater, A.; Duran, M.; Solà, M.; Benet-Buchholz, J. *Inorg. Chem.* **2006**, *45*, 10520–10529. (b) Poater, A.; Mola, J.; Gallegos Saliner, A.; Romero, I.; Rodríguez, M.; Llobet, A.; Solà, M. *Chem. Phys. Lett.* **2008**, *458*, 200–204. (c) Mola, J.; Romero, I.; Rodríguez, M.; Bozoglian, F.; Poater, A.; Solà, M.; Parella, T.; Benet-Buchholz, J.; Fontrodona, X.; Llobet, A. *Inorg. Chem.* **2007**, *46*, 10707–10716.